Patient-Specific Synthetic Osteochondral Resurfacing of an Extensive Shoulder OCD Lesion in a Dog

Sanja Sutalo[1] Michael Kühn[2] Peter Böttcher[1]

[1] Small Animal Clinic, FU-Berlin, Berlin, Germany
[2] Small Animal Clinic Panitzsch, Panitzsch, Germany

VCOT Open 2024;7:e11–e16.

Address for correspondence Peter Böttcher, MD vet., Klinik für Klein- und Heimtiere, Oertzenweg 19 b, 14163 Berlin, Germany (e-mail: peter.boettcher@fu-berlin.de).

Abstract

The aim of this study was to describe template-guided implantation and clinical outcome of a patient-specific resurfacing implant for an extensive humeral head osteochondritis in a client-owned dog. An 8-month-old intact female Irish Wolfhound, weighing 45 kg, exhibiting lameness in the right thoracic limb, and diagnosed with an extensive caudocentral humeral head osteochondritis. Based on computed tomography data, an anatomically contoured patient-specific implant (Ø 25 mm) was created. The implant consisted of a trabecular titanium base and a polycarbonate urethane bearing cup. For intraoperative guidance, a surgical drill guide, models of the affected humeral head, and trial implants were 3D printed. The implantation procedure was performed using the modified Cheli approach. Orthopaedic and radiographic follow-up examinations were conducted at 6 weeks and 10 months postoperatively. The examination revealed stable implant position, and some mild residual lameness at 6 weeks. Furthermore, the mild osteophytosis, initially evident on the day of surgery, showed a progression during each subsequent follow-up. Complications were not observed at any time point. At 10 months, the dog was free of lameness and exhibited no functional impairment, even after strenuous exercise. This level of activity remained unchanged up to the latest follow-up at 18 months, as confirmed during a telephonic interview. The utilization of a patient-specific resurfacing implant using a guided approach was technically feasible and resulted in excellent short- to mid-term clinical outcome in this case of extensive caudocentral humeral head osteochondritis dissecans (OCD) lesion. However, it is crucial to note that the potential influence of the implant on osteoarthritis progression requires further investigation.

Keywords
- osteochondritis dissecans
- shoulder joint
- resurfacing
- polyurethane
- patient specific
- navigation
- dog

Introduction

Osteochondritis dissecans (OCD) commonly affects the shoulder joint of immature medium-sized and large breed dogs. Bilateral involvement occurs in approximately 30% of cases. The caudal articular surface of the humeral head is the typical location for shoulder OCD, although the glenoid cavity of the scapula can be affected less frequently.[1–3] Surgical treatment, such as debridement via arthroscopy or arthrotomy, followed by stimulation of fibrocartilage formation, significantly improves clinical function.[4] However, persistent lameness has been reported, particularly when the lesion is located on the caudocentral aspect of the humeral head. In addition to surgical debridement and bone marrow stimulation techniques, alternative treatments such as osteochondral autograft or allograft transfer and synthetic osteochondral resurfacing of

received
July 7, 2023
accepted after revision
October 23, 2023

DOI https://doi.org/10.1055/s-0043-1778092.
ISSN 2625-2325.

Georg Thieme Verlag KG, Rüdigerstraße 14, 70469 Stuttgart, Germany

the humeral head have been reported in dogs.[5–8] The use of synthetic implants offers advantages, such as eliminating limitations associated with donor availability in case of allograft transplantation or the risk of significant donor site morbidity in autograft transfer. Synthetic implants have demonstrated good functional outcomes in the shoulder joint of affected dogs.[6,8] However, currently available synthetic resurfacing implants do not precisely match the local joint surface curvature, and this mismatch becomes more apparent with larger lesions, potentially impacting long-term functional outcome.

This case report describes the surgical technique and clinical outcome of a patient-specific resurfacing implant used to treat a large humeral head defect in a juvenile Wolfhound. The defect was deemed nonreconstructable using an off-the-shelf implant.[6,8]

Case Description

An 8-month-old intact female Irish Wolfhound weighting 45 kg was referred to the Small Animal Clinic of the Free University of Berlin, Germany, due to a 3.5-month history of grade III/V right thoracic limb lameness. Pain was elicited during the extension and flexion of the shoulder joint upon orthopaedic examination. Radiographic and computed tomography (CT) images confirmed the presence of an extensive OCD defect measuring 25 × 20 × 10 mm (length × width × depth), in the caudocentral region of the humeral head (►**Fig. 1**). Furthermore, an adjacent subchondral defect measuring 1 mm

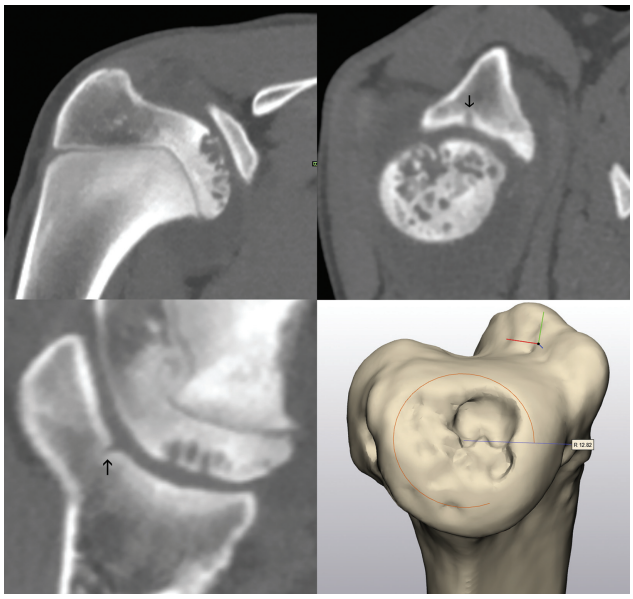

Fig. 1 Multiplanar computed tomography (CT) reformation and three-dimensional (3D) rendering of the affected right shoulder joint. The images highlight the extent of the osteochondritis dissecans (OCD) lesion (diameter ≥ 25 mm), which encompasses nearly the entire humeral head. Furthermore, there is notable involvement of the subchondral bone plate, underscoring the severity of the condition. The small subchondral defect within the glenoid fossa (*black arrows*) strongly indicates a subtle OCD like lesion that does not have clinical significance.

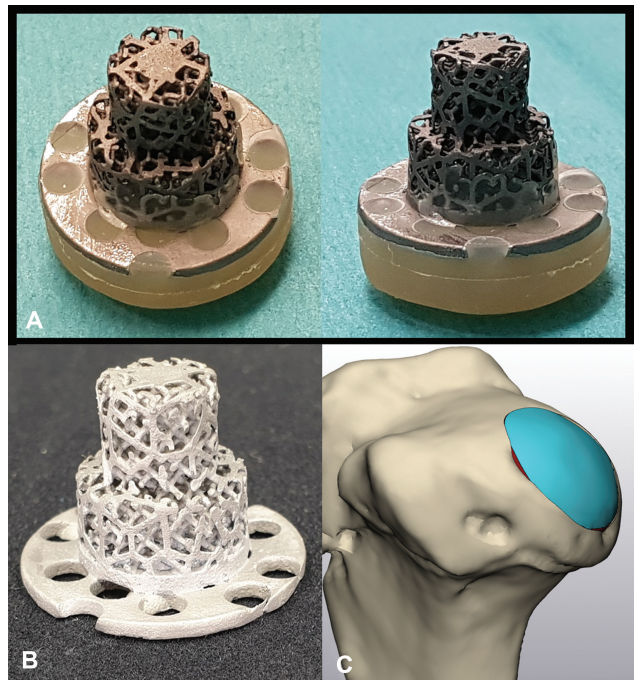

Fig. 2 Patient-specific, synthetic osteochondral resurfacing implant. (**A**) Bottom view of the original implant, featuring a titanium socket and a polycarbonate urethane bearing surface. (**B**) Titanium socket designed with an open pore trabecular structure to enhance bony anchorage. (**C**) Three-dimensional rendering demonstrating the implant's surface shape, mimicking the natural curvature of the humeral head.

was observed at the glenoid fossa, in contact with the cranial aspect of the humeral head lesion (*black arrows* in ►**Fig. 1**).

A 3D computer-aided design (CAD) model of the implant was constructed using specialized software (Mimics Innovation Suite, Materialise, Leuven, Belgium) based on the available CT images (►**Fig. 2**), using the unaffected humeral head as reference. A single cylindrical design with a diameter of 25 mm was selected to cover the entire lesion and simplify the surgical procedure by using only one central guide pin. The final implant comprised a trabecular like titanium base (►**Fig. 2B**) cast in medical-grade 4 titanium with a pore size of 1.5 mm. Additionally, a polycarbonate urethane (PCU) bearing cup (Carbothane AC-4085A, the Lubrizol Corporation, Wilmington, MA, United States) was incorporated, which was over-molded onto the titanium base.

For implantation, a patient-specific surgical drill guide was 3D printed (Form 2, Formlabs GmbH, Berlin, Germany). The drill guide, made from Formlab's "Surgical Guide" resin, securely locked onto the humeral head, ensuring precise alignment.

Surgery started with standard lateral shoulder arthroscopy using a 2.4-mm 30-degree fore-oblique arthroscope. A distinct irregularity was noted in the joint cartilage, aligning with the previously identified subchondral defect at the glenoid fossa. Furthermore, the osteochondritis cartilage flap on the humeral head was still in situ and centrally attached. Additionally, loose cartilage fragments and an 8 × 10 mm vascularized loose osteochondral fragment, which was wedged to the synovial membrane, were

visualized in the caudodistal joint pouch, accompanied by noticeable synovitis throughout the joint. All fragments were arthroscopically removed through a caudolateral working portal.

To gain optimal exposure for implantation, a modified Cheli approach was performed, with the shoulder positioned at maximum flexion.[9] As a modification of the standard Cheli approach, the joint capsule incision was extended caudally along the lateral glenoid rim until the humeral head could be luxated craniolaterally.[8] A blunt Hohman retractor within the joint space and two Gelpi retractors on the joint capsule provided complete visualization of the humeral head, allowing unrestricted access to the entire OCD lesion. Following debridement of the humeral head OCD lesion (►**Fig. 3A**), a 2.4-mm guide pin was placed at the center of the lesion using the 3D printed drill guide (►**Fig. 3B**), ensuring precise positioning and orientation of the guide pin as planned through computational modeling. Once the first guide pin was in place, the second 2.4-mm guide pin was inserted approximately 10 mm deep through the caudal drill tube to create the mark for rotational alignment of the implant (*arrow* in ►**Fig. 3B**). After removing the second guide pin as well as the drill guide, the recipient bed was prepared using a sequence of cannulated reamers with descending diameters, specifically 25, 15, and 10 mm (Arthrex VetSystem, Munich, Germany; ►**Fig. 3C,D**). The depth of reaming was controlled by the built-in collar of the reamers, serving as a depth limiter and a trial implant was used to verify proper preparation of the implant bed (►**Fig. 3E**). The patient-specific resurfacing implant was then inserted in a press-fit manner using a tamping tool (►**Fig. 4**). Visually, the implant appeared to restore the physiological curvature of the humeral head. Importantly, the transition between the weight-bearing surface of the implant and the surrounding joint cartilage was judged to be smooth, without palpable step formation. The joint was thoroughly irrigated, and precise reconstruction of the lateral joint capsule was performed, incorporating the embedded lateral glenohumeral ligament. The surgical site was closed using standard closure techniques. In the immediate postoperative phase, mediolateral radiographs and repeated axial CT imaging were acquired documenting correct placement of the implant (►**Fig. 5A,B**), except for a minimal gap between the host bone and the bottom surface of the titanium base.

The dog was discharged on the same day with robenacoxib (1 mg/kg orally by mouth every 24 hours for 10 days). Strict rest and controlled exercise were advised for the initial 6-week period. Regular physical therapy began 10 days after surgery with mild passive range-of-motion exercises and was supplemented over the following 5 weeks with exercises focusing on balance and strength. The dog began bearing weight on the limb 5 days postsurgery, exhibiting a grade III/V lameness. On the day of suture removal, 10 days after surgery, the surgical wound had healed without complications.

Recheck examinations, including visual gait analysis, orthopaedic examination, and shoulder radiographs, were

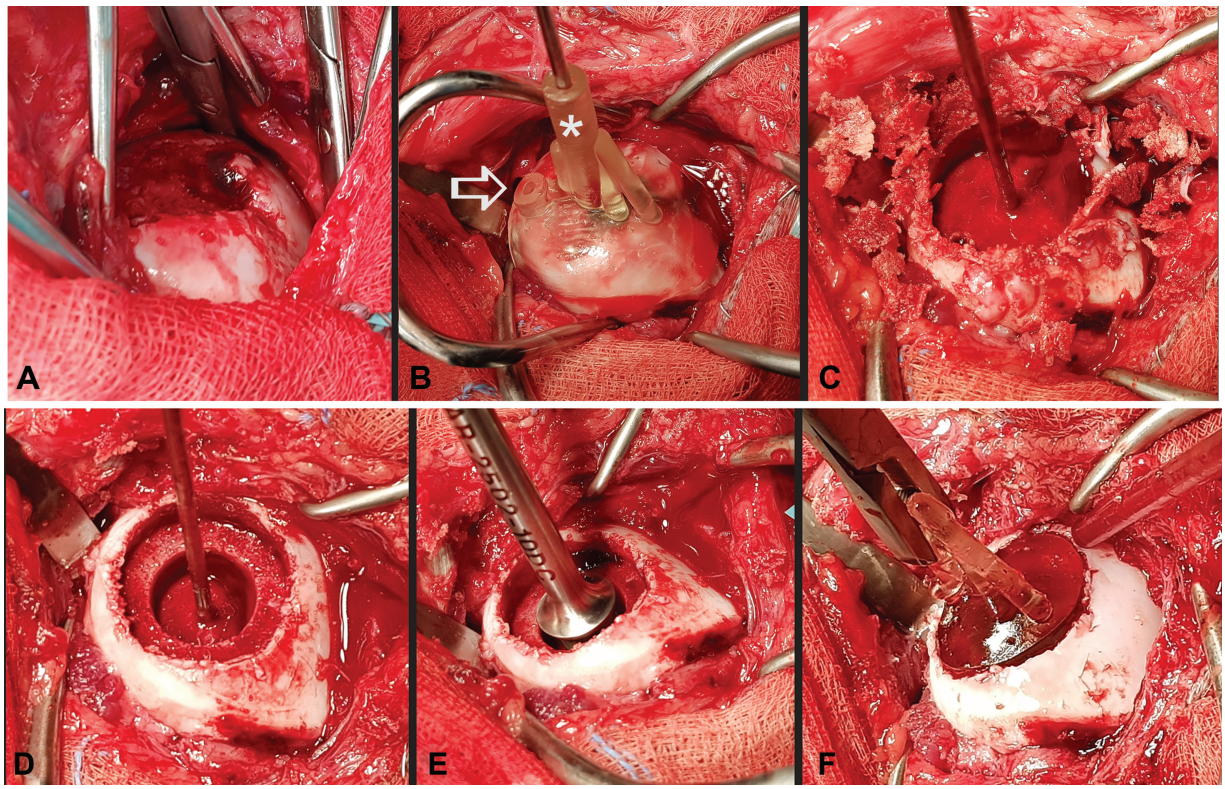

Fig. 3 Consecutive steps during preparation of the implant bed (view from proximolateral, cranial to the right). (**A**) Exposure of the humeral head with debridement of any loose cartilage. (**B**) Placement of the central guide pin (*asterisk*) using the surgical template. The caudal tube defines the rotational alignment mark (*arrow*). (**C–E**) Reaming of the implant bed with cannulated reamers of decreasing diameter (25, 15, and 10 mm) and build-in depth limiter. (**F**) Placement of the trial implant to confirm proper preparation of the implant bed.

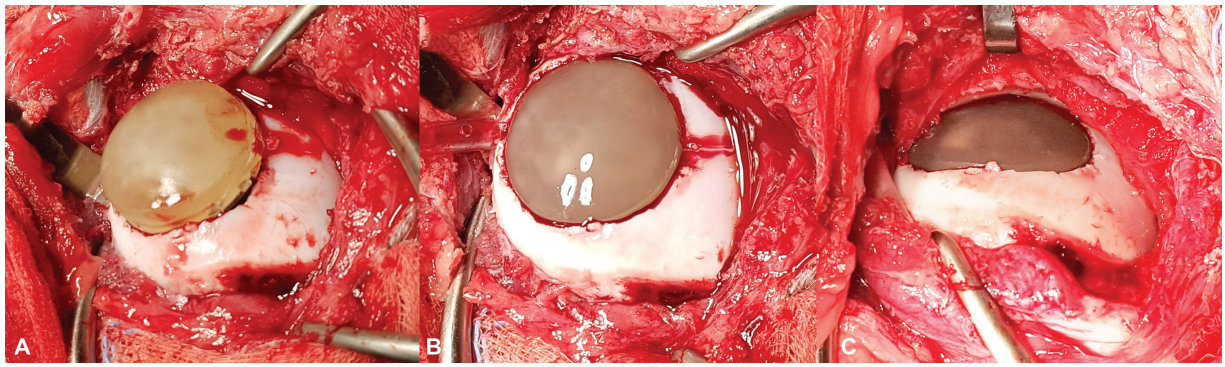

Fig. 4 Placement of the patient-specific synthetic resurfacing implant (proximolateral view, cranial to the right). (**A**) The implant was initially positioned manually, aligning the reference point at the titanium socket with the previously established rotational alignment landmark. (**B**,**C**) The implant after impaction and press-fit anchorage, demonstrating restoration of physiological curvature of the humeral head. Observe the smooth transition between the weight-bearing surface of the implant and the surrounding joint cartilage, indicating proper positioning without any palpable step formation.

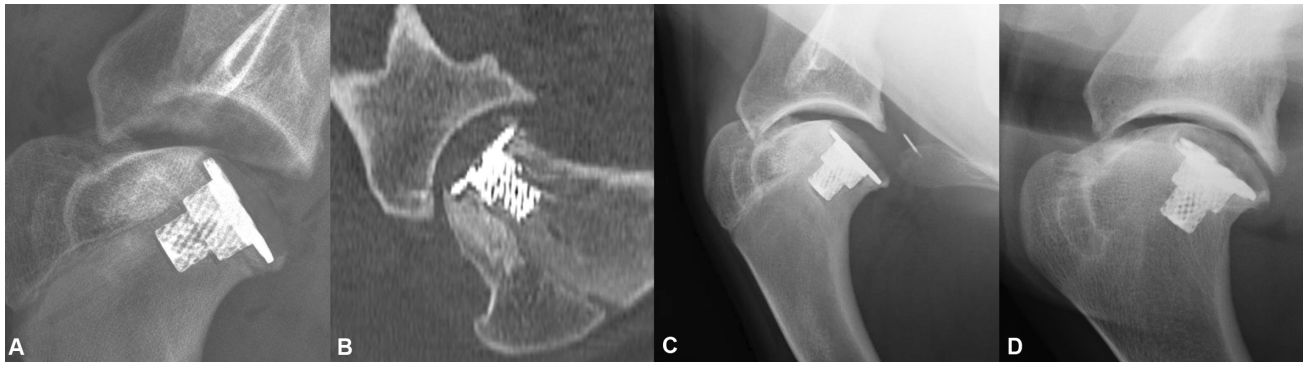

Fig. 5 Radiographic and computed tomography (CT) follow-up imaging. (**A**,**B**) Immediate postoperative imaging documenting placement of the implant with some minimal gap between the host bone and the bottom surface of the titanium base. Note the preexisting osteophytosis within the bicipital groove as well as at the caudal glenoid rim. (**C**) At the 6-week mark, the implant position remains unchanged. Incomplete bonding of the host bone to the implant socket is observed, characterized by persistent gap formation caudally and distally. Osteophyte size has slightly increased. (**D**) At 10 months, gap healing is achieved. The implant appears stable and appropriately positioned. Radiographic signs of osteoarthritis have further increased.

conducted at 6 weeks and 10 months postoperatively. At the 6-week examination, only a grade I/V lameness was observed, and manipulation of the shoulder joint elicited no pain response. Radiographic follow-ups (►**Fig. 5C,D**) revealed progression of osteophytosis at the supra- and infraglenoid tubercles and within the bicipital groove 6 weeks after implantation. The gap between the host bone and the bottom surface of the titanium base was still incompletely filled with bone. At 10 months, the gap had disappeared, indicating bonding of the titanium socket and the surrounding host bone. At that time, the dog was free of lameness and exhibited no functional impairment, even after strenuous exercise. During a telephonic follow-up interview at 18 months, the owners reported normal limb function without any restrictions.

Discussion

This case report describes the successful template-guided resurfacing of a large caudocentral OCD lesion on the humeral head using a synthetic patient-specific resurfacing implant. The procedure resulted in good limb function and no minor or major complications during the 18-month follow-up period. The decision to explore alternative treatment options to traditional surgical debridement and fibrocartilage healing was based on the extensive size and central location of the lesion, which typically present a guarded functional prognosis.[4] Because the commercially available resurfacing implants would not restore the physiological joint surface curvature of the extensive lesion in the presented case, a patient-specific implant was chosen. Template-guided implantation in osteochondral resurfacing has shown to significantly improve the geometrical accuracy of the reconstructed surface, in both ex vivo and in vivo settings,[10,11] while also being cost-effective and straightforward to implement intraoperatively. Through the combination of a patient-specific implant and template-guided surgery, we enhanced the probability of achieving anatomical resurfacing, a result that met our expectations.

Due to the increased curvature and elevation of the weight-bearing surface of the anatomically shaped implant, which exposes it to higher pivoting forces during joint loading compared with flat standard implants, the socket was designed to sit deeper in the host bone (25 vs. 8 mm),

enhancing implant stability. However, the potential concern of penetrating the epiphyseal growth plate and affecting bone growth and surface shaping of the humeral head during residual growth should be considered in very young dogs undergoing the procedure.

Although impaction of the implant did not result in full contact between the host bone and the bottom of the implant socket and gap healing was still lacking in some areas at 6 weeks postoperatively, complete bone-to-implant contact was present at the 10-month recheck. This is consistent with findings in sheep that underwent synthetic osteochondral resurfacing, where bone-to-implant contact bonding was observed as early as 6 months.[12] Most likely slight kinking of the implant during impaction or some minimal inaccuracy during reaming may have resulted in incomplete seating in the present case.

Polycarbonate urethane was chosen as the surface layer, due to its chemical and physical stability, similar modulus of elasticity to cartilage, high wear resistance, and overall bearing properties resembling native joint surfaces.[13–15] This material has been shown to induce minimal damage to adjacent normal hyaline cartilage in typical unipolar OCD resurfacing settings, with almost no detectable wear or fatigue.[14,16]

The presence of cartilaginous changes at the center of the glenoid fossa seen during arthroscopy may raise concerns about using polycarbonate urethane as a bearing surface, as implant wear may be higher in the presence of osteoarthritis changes.[17] Alternatively, a full metal implant could be considered, but it might result in accelerated damage to the glenoid fossa,[18] making it a less favorable option compared with the chosen implant configuration. Given that the cartilage changes at the glenoid fossa resemble an "OCD-like" lesion rather than typical osteoarthritic changes,[19] the potential wear of the polyurethane implant is presumed to be minimally elevated, if elevated at all. Due to the limited extent of cartilage damage and marginal subchondral involvement, no surgical debridement of the lesion was performed.

The obvious progression of radiographic signs of osteoarthritis, primarily marked by the advancement of preexisting osteophytosis, raises concerns regarding the efficacy of the presented treatment approach, particularly in the long term. Currently, there are insufficient data available to conclusively attribute the progression of osteoarthritis to specific factors, such as potential implant malfunction, the invasiveness of the surgical approach, or the intrinsic joint pathology, which was already present prior to the surgery and is inherently irreversible through the procedure. Further investigations are necessary to evaluate the long-term implications of the chosen treatment modality and to assess its impact on joint function and stability.

Limitations of this case report include the lack of objective gait analysis, second-look arthroscopy, and long-term follow-up. Direct examination of the implant surface, adjacent cartilage, articulating glenoid cartilage, and synovium could reveal implant-associated complications, such as local inflammation, wear, septic/aseptic loosening, or damage to the opposing cartilage that may not be noticeable solely on physical examination and radiography.

Nonetheless, the favorable assessment of comparable implant systems used in the stifle and shoulder joints of dogs, with a maximum follow-up of 4.2 years,[6,20] serves as a compelling indicator of their potential for long-term functionality.

This case report describes the successful resurfacing of a sizable osteochondral lesion located in the caudocentral region of the humeral head. The procedure involved the utilization of a patient-specific synthetic anatomical resurfacing implant, complemented by intraoperative guidance using a surgical template. As a result, the physiological humeral head topography was restored, and joint function promptly returned without any indications of complications in the short to midterm.

Funding
None.

Conflict of Interest
None declared.

References

1 Craig PH, Riser WH. Osteochondritis dissecans in the proximal humerus of the dog. J Am Vet Radiol Soc. 1965;6:40–49
2 Slater MR, Scarlett JM, Kaderly RE, et al. Breed, gender, and age as risk factors for canine osteochondritis dissecans. Vet Comp Orthop Traumatol 1991;4:100–106
3 LaFond E, Breur GJ, Austin CC. Breed susceptibility for developmental orthopedic diseases in dogs. J Am Anim Hosp Assoc 2002; 38(05):467–477
4 Olivieri M, Ciliberto E, Hulse DA, Vezzoni A, Ingravalle F, Peirone B. Arthroscopic treatment of osteochondritis dissecans of the shoulder in 126 dogs. Vet Comp Orthop Traumatol 2007;20(01):65–69
5 Fitzpatrick N, van Terheijden C, Yeadon R, Smith TJ. Osteochondral autograft transfer for treatment of osteochondritis dissecans of the caudocentral humeral head in dogs. Vet Surg 2010;39(08): 925–935
6 Murphy SC, Egan PM, Fitzpatrick NM. Synthetic osteochondral resurfacing for treatment of large caudocentral osteochondritis dissecans lesions of the humeral head in 24 dogs. Vet Surg 2019; 48(05):858–868
7 Franklin SP, Stoker AM, Murphy SM, et al. Outcomes associated with osteochondral allograft transplantation in dogs. Front Vet Sci 2021;8:759610
8 Danielski A, Farrell M. Use of synthetic osteochondral implants to treat bilateral shoulder osteochondritis dissecans in a dog. Vet Comp Orthop Traumatol 2018;31(05):385–389
9 Vezzoni A, Vezzoni L, Boiocchi S, Miolo A, Holsworth IG. A modification of the Cheli craniolateral approach for minimally invasive treatment of osteochondritis dissecans of the shoulder in dogs: description of the technique and outcome in 164 cases. Vet Comp Orthop Traumatol 2021;34(02):130–136
10 Kunz M, Devlin SM, Hurtig MB, et al. Image-guided techniques improve the short-term outcome of autologous osteochondral cartilage repair surgeries: an animal trial. Cartilage 2013;4(02): 153–164
11 Sebastyan S, Kunz M, Stewart AJ, Bardana DD. Image-guided techniques improve accuracy of mosaic arthroplasty. Int J CARS 2016;11(02):261–269
12 Martinez-Carranza N, Ryd L, Hultenby K, et al. Treatment of full thickness focal cartilage lesions with a metallic resurfacing

implant in a sheep animal model, 1 year evaluation. Osteoarthritis Cartilage 2016;24(03):484–493
13 Khan I, Smith N, Jones E, Finch DS, Cameron RE. Analysis and evaluation of a biomedical polycarbonate urethane tested in an in vitro study and an ovine arthroplasty model. Part I: materials selection and evaluation. Biomaterials 2005;26(06):621–631
14 Khan I, Smith N, Jones E, Finch DS, Cameron RE. Analysis and evaluation of a biomedical polycarbonate urethane tested in an in vitro study and an ovine arthroplasty model. Part II: in vivo investigation. Biomaterials 2005;26(06):633–643
15 Kanca Y, Milner P, Dini D, Amis AA. Tribological evaluation of biomedical polycarbonate urethanes against articular cartilage. J Mech Behav Biomed Mater 2018;82:394–402
16 Cook JL, Kuroki K, Bozynski CC, Stoker AM, Pfeiffer FM, Cook CR. Evaluation of synthetic osteochondral implants. J Knee Surg 2014; 27(04):295–302
17 Damen AHA, Nickien M, Ito K, van Donkelaar CC. The performance of resurfacing implants for focal cartilage defects depends on the degenerative condition of the opposing cartilage. Clin Biomech (Bristol, Avon) 2020;79:105052
18 Custers RJH, Dhert WJA, Saris DBF, et al. Cartilage degeneration in the goat knee caused by treating localized cartilage defects with metal implants. Osteoarthritis Cartilage 2010;18(03): 377–388
19 Lande R, Reese SL, Cuddy LC, Berry CR, Pozzi A. Prevalence of computed tomographic subchondral bone lesions in the scapulohumeral joint of 32 immature dogs with thoracic limb lameness. Vet Radiol Ultrasound 2014;55(01):23–28
20 Egan P, Murphy S, Jovanovik J, Tucker R, Fitzpatrick N. Treatment of osteochondrosis dissecans of the canine stifle using synthetic osteochondral resurfacing. Vet Comp Orthop Traumatol 2018;31 (02):144–152